Journal of Geosciences and Geomatics, 2023, Vol. 11, No. 1, 11-20
Available online at http://pubs.sciepub.com/jgg/11/1/2
Published by Science and Education Publishing
DOI:10.12691/jgg-11-1-2

Updated Atmospheric Modelling of Refracted Zenith Angle Using Vertical Temperature Gradient for Refraction Coefficient

Mansoor Sabzali*, Lloyd Pilgrim

Department of Civil, Surveying and Environmental Engineering, University of Newcastle, Callaghan, New South Wales, Australia
*Corresponding author: mansoor.sabzali@newcastle.edu.au

Received February 22, 2023; Revised March 27, 2023; Accepted April 07, 2023

Abstract The atmosphere is an undeniable source of error for geodetic observations which cannot be underestimated or controlled by surveyors in the fieldwork measurements. Technicians using total stations and laser scanners require to have an accurate zenith angle measurement in order to accurately determine the 3D coordinates of points. Therefore, having a thorough knowledge of atmospheric influencing the zenith angle measurements is important. Terrestrial surveying instruments typically use a laser in the domain of visible light or near-infrared in the electromagnetic spectrum. The deviation is introduced by the different intersecting angles between the laser beam and the various atmospheric layers. The phenomenon is called the refractivity of waves. Snell's law can be used to calculate the deviation of the laser as it moves through different layers of the atmosphere. This study aims to develop an understanding of the refractivity on zenith angle under the local refraction coefficient via considering vertical temperature gradient (VTG) as its major contributing factor into the assumed layers of atmosphere above the Earth's surface, where the geodetic measurements might take place. The coefficient is also dependent on the other observable atmospheric elements such as temperature, pressure, and humidity. However, the accurate knowledge of VTG is not a straightforward task due to an inability to obtain direct measurements and its unexpected fluctuations. Consequently, the proper modelling of VTG through simulated and real datasets analyses with the aid of mathematical least square approach is pursued to achieve an updated atmospheric model for refracted zenith angle.

Keywords: *electromagnetic spectrum, least square, local refraction coefficient, refracted zenith angles, updated atmospheric modelling, vertical temperature gradient*

Cite This Article: Mansoor Sabzali, and Lloyd Pilgrim, "Updated Atmospheric Modelling of Refracted Zenith Angle Using Vertical Temperature Gradient for Refraction Coefficient." *Journal of Geosciences and Geomatics*, vol. 11, no. 1 (2023): 11-20. doi: 10.12691/jgg-11-1-2.

1. Introduction

The uncertainty (accuracy) of all laser-based instruments is highly dependent on the accuracy of the propagating wavelength and its velocity. Any electromagnetic wave moving through the atmosphere is affected by different components of the atmosphere including:

i. air temperature,
ii. the atmospheric pressure of air,
iii. water vapour of air (humidity),
iv. the effects of carbon dioxide content,
v. oil vapour of air, and
vi. the effects of an absorption line in the air.

Each of the above cause different variations in the velocities of the wave propagating into different mediums of the atmosphere and change the direction of travel of the wave in order to follow the quickest path. This phenomenon is explained by Fermat's principle and the associated Snell's law as follows:

Electromagnetic waves can be described by wavelength $\lambda(m)$, frequency $f(Hz)$ and propagation velocity $v(\mathrm{m/s})$. The relationship is defined [1]:

$$\lambda = \frac{v}{f} \tag{1}$$

Therefore, the relationship of propagating velocity of a wave into air $v(\mathrm{m/s})$ compared to the velocity of the same wave propagating in a vacuum (299792458m/s), will be defined by the refractive index n, and the associated property refractivity N is given by:

$$n = \frac{c}{v} \tag{2}$$

$$N = (n-1)\times 10^6 \tag{3}$$

Both n and N are unitless values.

Assuming refractive index of n in Equation 2, it can be resolved into two components of horizontal and vertical elements:

$$n = \frac{\partial n}{\partial x}\vec{i} + \frac{\partial n}{\partial h}\vec{k} \quad (4)$$

Where $\frac{\partial n}{\partial x}$ is horizontal gradient of refractive index (horizontal refraction (HR)) which is not the scope of this work, and $\frac{\partial n}{\partial h}$ is vertical gradient of refractive index (vertical refraction (VR)) (m^{-1}) (will be discussed in next Section).

Each component varies the directions in their corresponding surfaces separately [2,3].

Figure 1 illustrates the effect of the refraction of air on a propagating wave, where δs is the apparent path length, ds is the straight-line path - also called real path (chord), z is measured zenith angle, and dz is refracted zenith angle.

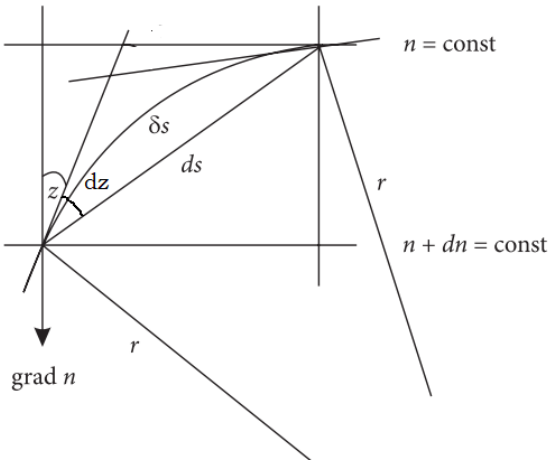

Figure 1. Refraction [4]

In the real-world scenario, refraction on zenith angle measurements can occur in two different cases which eventually leads to the bending of the measuring beam and the resulting refracted zenith angles.

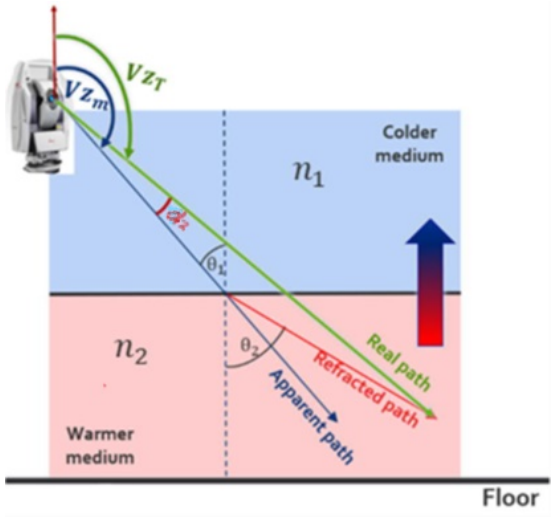

Figure 2. Refraction on zenith angle (n_1>n_2) [5]

First, if the ray goes from a denser air layer to a less dense air layer, the result is a concave curvature of the wave path, (i.e., the opposite to the Earth's curvature (Figure 2)). This scenario normally occurs on sunny days when the radiation of the Sun during the day is severe and trapped into the atmosphere.

Here, indices m and T refer to measured and corrected (non-refracted) zenith angle, respectively, and dz is defined as refracted zenith angle [5].

The second case is the reverse condition (i.e., the wave travels from the less dense layer into the denser layer. The convex curvature of the path as it follows the Earth's curvature is shown in Figure 3).

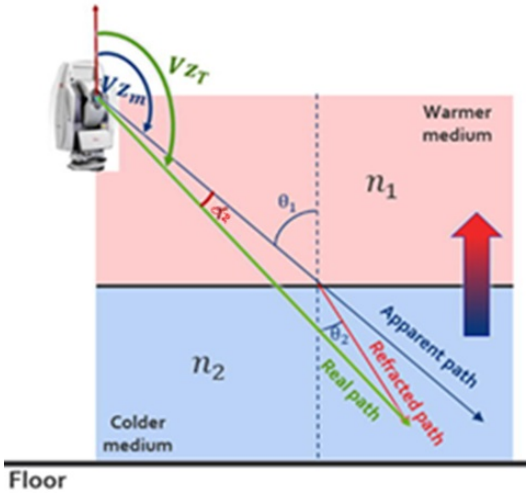

Figure 3. Refraction on zenith angle (n_2>n_1) [5]

It is obvious that refracted zenith angle dz can be positive (Figure 3) or negative (Figure 2) depending on whether there is a concave and convex bending of the rays.

2. Literature Review

The refracted zenith angle is introduced based on the bending wave (Figure 2 and Figure 3) which is deviated from its own way as the result of atmospheric influences. Thus, the review here contains following steps prior to understanding the refracted zenith angle:

i. refraction coefficient k (dimensionless value) and its relationship with vertical refraction (VR) $\frac{\partial n}{\partial h}$ (m^{-1}),
ii. laboratory simulated setup for computation of vertical temperature gradient (VTG) $\frac{\partial T}{\partial h}$ $(°K/m)$,
iii. approximations of VTG and VR in different layers of atmosphere by other scientists, and finally
iv. refracted zenith angle dz (rad) and its correction C_R on z coordinate (m). Hereafter, in order to separate between the correction C_R on coordinate z and zenith angle z, we define only correction C_R.

2.1. Refraction Coefficient and Its Relationship with Vertical Refraction

Reference [4] proved that the quantification to recognise the direction of the bending ray on vertical

plane is expressed by the term called the coefficient of refraction k (i.e., it is a dimensionless value). To determine this coefficient, there have been different proposals throughout the years. The most prominent methods are:

- Measurement of the vertical temperature gradient (VTG) as the main influential factor [6].
- Incorporation of atmospheric effects into the adjustment process of geodetic networks [7].
- Special measuring procedures such as mutual-simultaneous observations or symmetrical observation configurations [1].
- Dual-wavelength methods utilizing atmospheric dispersion to derive the refraction angle from the dispersion angle [8].
- Turbulent transfer model (TTM) using the upward sensible heat flux for deviation of the temperature gradient [9].

The applied method to recognize the refraction coefficient is the estimation of VTG as its major factor.

From a geometric perspective, the coefficient of refraction k is defined as the ratio of the mean radius of the Earth R $(= 6371000\ m)$, to the refraction radius of the curvature of light path r (m) (Figure 1) [4].

$$k = \frac{R}{r} \tag{5}$$

Theoretically speaking, under the normal atmospheric conditions, [4,10] have verified the general atmospheric value for refraction coefficient, based on Gaussian distribution, is approximately +0.13 in the validation of their calculation in the Hanover geodetic network. The correction for geodetic refraction based on this value was calculated as $\frac{1}{7}$ of the correction of the curvature of Earth, with the mean value of Earth's radius and average refraction radius of the circular path of light about $49\times10^6 m$. This is the common value which numerous terrestrial surveying instruments automatically apply to zenith angle measurements. Further details are found in [4,7,10]

On the other hand, the refraction radius of the curvature of light path r is proportional to vertical gradient of refractive index (vertical refraction) $\frac{\partial n}{\partial h}$, and z zenith angle.

$$\frac{1}{r} = -\left(\frac{\partial n}{\partial h}\right)\sin z \tag{6}$$

Therefore, from two Equations above, the coefficient of refraction is given by:

$$k = -R\left(\frac{\partial n}{\partial h}\right)\sin z \tag{7}$$

To determine the vertical gradient of refractive index, [11] modelled the refracted range based on former refractive index models. For example, one of the proposed models adopted by (International Association of Geodesy [IAG], called Closed Formulae 1999 [12]) is as follows:

$$N(\lambda) = \left(n(\lambda)-1\right)\times10^6 = 287.6155 + \frac{4.8866}{\lambda^2} + \frac{0.068}{\lambda^4} \tag{8}$$

$$(n-1)\times10^6 = \frac{273.15N(\lambda)P}{1013.25T} - \frac{11.27e}{T} \tag{9}$$

Here, $N(\lambda)$ and $n(\lambda)$ are group refractivity and refractive index resp. as a function of wavelength λ (μm), P is the atmospheric pressure $(mbar)$, T is temperature (^0K), and e is partial pressure vapour relating to humidity $(mbar)$. There are numerous other models investigated in detail by [11].

By substitution of two Equations above, and inserting corresponding wavelength which is here assumed in the light domain of electromagnetic wave (EM) (e.g., $0.658\ \mu m$), refractive index is given by:

$$n = \left[\left(76\frac{P}{T} - \frac{11.27e}{T}\right)\times10^{-6}\right] + 1 \tag{10}$$

The vertical gradient of refractive index is our interest. Therefore,

$$\frac{\partial n}{\partial h} = \left[\frac{76}{T}\frac{\partial P}{\partial h} + \left(\frac{11.27e}{T^2} - \frac{76P}{T^2}\right)\frac{\partial T}{\partial h} - \frac{11.27}{T}\frac{\partial e}{\partial h}\right]\times10^{-6} \tag{11}$$

Where, $\frac{\partial T}{\partial h}$ is the vertical gradient of temperature which is the main concern of this research $(^0K/m)$, $\frac{\partial P}{\partial h}$ is vertical gradient of pressure which is computed by [13]:

$$\frac{\partial P}{\partial h} = -\frac{g}{M}\frac{P}{T} \tag{12}$$

Here, $g = 9.81\ m/s^2$ is the gravitational acceleration, and $M = 28.7\ m^2/{}^0K\ s^2$ is the specific gas constant for dry air. The numerical value for coefficient $\frac{g}{M}$ is $0.0342\ ^0K/m$.

In the third term, vertical gradient of partial vapour pressure $\frac{\partial e}{\partial h}$ is quite negligible, and in standard condition of air defined by [1] is less than 2% of $\frac{\partial P}{\partial h}$ which can be neglected [2].

Therefore, the simplified Equation 11 for vertical gradient of the refractive index is then given by:

$$\frac{\partial n}{\partial h} = -\frac{P}{T^2}(76)\left[0.0342 + \left(\frac{\partial T}{\partial h}\right)\right]\times10^{-6} \tag{13}$$

From the Equations 7 and 13, and the substitution of R and maximum zenith angle at horizon $(z = 90)$, refraction of coefficient will be as follows:

$$k = 484.12\frac{P}{T^2}\left[0.0342 + \left(\frac{\partial T}{\partial h}\right)\right] \tag{14}$$

From a practical point of view, it can be inferred that, with assumption of constant vertical temperature gradient,

the magnitude of the refraction coefficient is least in the middle hours of the day when the temperature reaches its highest and highest height above mean sea level (MSL) due to the lower pressure. However, VTG regards its variations as seasonal (i.e., it is least in the springtime of the year when it is the most favourable time for angle measurements [14,15,16]).

The main difficulty of Equation 14 is vertical temperature gradient where an accurate understanding of its magnitude in the various layers of atmosphere is not a straightforward task. Furthermore, no existing optical devices can sense this meteorological influence. Thus, it will be the natural motivation of this current update.

2.2. Laboratory Simulated Setup for VTG

Equation 14 depicts the refraction coefficient is related to the variation of atmospheric conditions and VTG. It is achievable to observe the temperature and pressure of the measurement environment; however, the VTG is the main burden in real time measurement due to the fact that there could be no sensors available to directly observe the VTG in the field. Hence, there have been several measurements models presented by different scientists throughout years to estimate VTG under controlled laboratory conditions. A number of key models are provided in Table 1. (i.e., vertical temperature gradient functions are those describing the relation of the air temperature T (^0K) to the height above the ground h (m)).

Table 1. Some of existing functions to calculate vertical temperature gradient (VTG)

Functions	Temperature w.r.t Height	Temperature Gradient* ($\frac{dT}{dh}$)
Kukkamaki (1938) [17]	$a + bh^c$	$b\ c\ h^{c-1}$
Reissman (1954) [18]	$a + bh + ch^2$	$b + 2\ c\ h$
	$a + bh + ch^2 + fh^3$	$b + 2\ c\ h + 3fh^2$
	$a + bh + ch^2 + fh^3 + gh^4$	$b + 2\ c\ h + 3fh^2 + 4gh^3$
Heer (1984) [19]	$a + be^{ch}$	$b\ c\ e^{ch}$
Kharagani (1987) [13]	$ah + b\ h^c$	$a + b\ c\ h^{c-1}$
Linear	$ah + b$	a

* Temperature gradient is the first derivation of functions w.r.t height ($^0K/m$).

The coefficients of a, b, c, f and g (provided in the Table 1) vary with time, and they can be calculated with the use of real observations of temperature above the ground.

One of the prominent laboratory methods to calculate the coefficients proposed by [13] is called the distribution of the temperature sensors on the rod. In short, this approach works as follows:

If using three temperatures sensors t_1, t_2 and t_3 at different heights arranged on rod above the ground h_1, h_2 and h_3 ($h_3 \leq 3\ m$), and the heights are configured such that $\frac{h_1}{h_2} = \frac{h_2}{h_3}$, then the following relationships hold [13],

$$\Delta T_1 = T_2 - T_1 \tag{15}$$

$$\Delta T_2 = T_3 - T_2 \tag{16}$$

and $\boldsymbol{b}$ and $\boldsymbol{c}$ are calculated by:

$$c = \frac{\ln\left(\frac{\Delta T_2}{\Delta T_1}\right)}{\ln\left(\frac{h_2}{h_1}\right)} \tag{17}$$

$$b = \frac{\Delta T_1}{z_2^c - z_1^c} \tag{18}$$

There could be the possibility to calculate the other constants f and g at higher heights than 3 m. Additionally, there is no serious requirement to take the calculation of a into account (i.e., except for the linear function) since it does not play an active role in the temperature gradient calculations in most of the functions given above in table.

2.3. Approximations of VTG and VR in Different Atmospheric Layers

To explore the findings of different scientists regarding estimations of VTG, it is recommended to categorise layers of the atmosphere into five layers in terms of the height from the Earth's surface: ultra-lowest (0 to 1 m), lowest (1 to 3 m), intermediate (3 to 20 m), highest (20 to 100 m), and ultra-highest (over 100 m) atmospheric layers.

Ultra-lowest atmosphere: Reference [20] demonstrated that refraction effects in the lowest atmosphere generally multiply with decreasing height. Further, [13] later acknowledged this layer experiences the extreme values of refraction, especially at the heights of a few tenths of a metre above the ground. This is because heat transition from the Earth's surface is the stronger, the less distant the atmospheric layers are. Therefore, the largest absolute values of temperature gradients are to be expected immediately above the ground. On the basis of temperature measurements, [20] computed possible variations of the refraction coefficient caused by variation of VTG which is able to reach between -47 and $+20\ ^\circ K/m$ directly above the ground. Close to the ground at 50 cm height, refraction coefficients were observed in the range between -8 and $+16$ on sunny days [21]. Reference [13] also showed extreme values of refraction coefficients of about -6 to -10 at heights of a few tenths of a meter above the ground. Hence, it is worthwhile to mention the geodetic measurements in ground clearance of 50 cm and lower should generally be avoided [22] which is likely since the measurement configuration due to the height of instrument would be over 1 m (lowest atmosphere).

Lowest atmosphere: This atmosphere is also called near-ground layer which is defined up to 3 m above the surface of Earth. Reference [13] obtained the value of vertical temperature gradient varying between -0.4 and $+0.2\ ^0K/m$ for typical near-ground surveying measurements. Over the day, the Sun's radiation is absorbed by Earth's surface leading to heating of the lowest atmospheric layers resulting in negative VTG, whereas, in the evening, the Earth's surface normally cools resulting in positive VTG. Although before [13], several scientists [20,21] calculated VTG at different heights, their approximations are close to Kharagani's values [22].

Intermediate atmosphere: The other layer of the atmosphere is from 3 to 20 m (intermediate surface) and is subjected to the same varying thermal properties as the lower layer with lesser interactions [14]. In this layer, over the day, the Sun's radiation is being absorbed by Earth's surface, and the warm terrain, in turn, heats up the lowest atmospheric layers, resulting in negative VTG of about $-0.5\ ^0K/m$ derived from practical temperature measurements [23]. Given Equation 14, the local coefficient is not only stronger but also concave curvature similar to two previous layers. Similar to the lower layer, in the evening, the Earth's surface normally cools off faster than the overlaying air strata. Usually, this results in strong positive gradients [14].

Highest atmosphere: The next layer is the highest atmosphere which starts from 20 to 100 m which is weakly influenced by the temperature of the surface, in contrast to the lower atmospheres and characterized by the VTG frequently about $-0.01\ ^0K/m$ [2]. The Gaussian refraction of coefficient which is approximately $+0.13$ [4,10] is computed for this layer which is the refraction for a majority of surveying instruments by default (i.e., positive magnitude for local refraction coefficient depicts the convex curvature of the path). In this research, it will be revealed that this value is certainly not reliable.

Ultra-highest atmosphere: For over 100 m height of Earth's surface, [2,4] studies in 1980 and 2001, respectively, showed VTG is about $-0.006\ ^0K/m$ (i.e., the decrease of 6 ^0K per kilometre height difference).

It is notable that there is another recognised surface by meteorological scientists over ice and water, in contrast to the vegetated ground surface discussed here. Both surfaces significantly differ in terms of their thermal properties usually resulting in an amplification of the refraction effect (refer to [22]).

2.4. Refracted Zenith Angle and Its Correction

Finally, after revealing the refraction of coefficient, the refracted zenith angle dz in rad is simply computed according to slope distance of S to each target point (chord) or non-refracted range (m) [2]. Non-refracted range is the corrected range having eliminated refractivity effects [11].

$$dz = \frac{Sk}{2R} \tag{19}$$

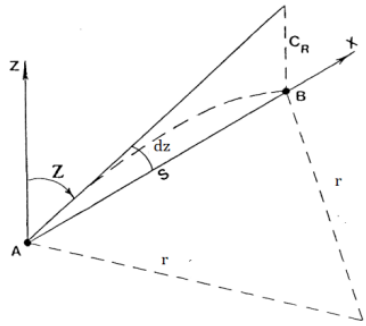

Figure 4. Refraction [13]

Then, non-refracted (corrected) zenith angle is then computed as follows:

$$z_{non-refracted\ OR\ corrected} = z + dz \tag{20}$$

The sign of the refracted angle depends on the bending path of the wave in which the optical ray travels from the instrument to the target as it has already been illustrated (Figure 2 and Figure 3). When the local refraction coefficient is negative depending on the direction of VTG, the amount of refraction angle should be subtracted from the measured ones (Figure 2). Otherwise, this amount should be added (Figure 3).

The correction from refracted zenith angle in meters will be also given by [2] (Figure 4):

$$C_R = -\frac{S^2 k}{2R} \tag{21}$$

In summary, Equation 14 indicates that every minor change in the atmospheric conditions leads to a variation in local coefficient refraction, and that variation w.r.t the corresponding slope distance to each target determines the refracted zenith angle and corresponding correction (Equations 20 and 21).

3. Methodology

As illustrated above, the change in refracted zenith angle caused by the variation in atmospheric parameters will be calculated if vertical temperature gradient is known in each layer where the measurement is taken place. But the direct observation of VTG is not possible during the field measurement. Therefore, on the one hand, the approach here is to determine the approximated refracted zenith angle and corresponding corrections from the estimations of VTG for each defined layers on simulated datasets (mentioned in Section 2.3), and, on the other hand, the real datasets consist of calculation of the exact value of VTG under uncontrolled environment of field observations through Least Square Adjustment (LSA) via the redundant angle observations and real observations of atmospheric conditions. Finally, updated refraction coefficient to mitigate the refracted zenith angle and its correction will be concluded.

3.1. Simulated Datasets

Two atmospheric parameters such as air temperature and atmospheric pressure, individually and simultaneously, will be considered within the standard range of atmospheric conditions expressed by [24,25] due to the applicability of certified surveying instruments. As argued earlier, the effect of humid air variation on zenith angle is insignificant and independent of the temperature gradient (Equation 14).

3.1.1. Air Temperature Analysis

In this analysis, the atmospheric pressure P is kept as a constant value and temperature T is increased, (by a step size of 5 ℃). The temperature range analyses are assumed from -5 to 45 ℃ since it regards to the atmospheric conditions of Newcastle, New South Wales in Australia[1] where the simulated and real datasets were acquired (in

1 http://www.meteorology.com.au/local-climate-history/nsw/newcastle http://www.bom.gov.au/akamai/https-redirect.html

the vicinity of University Newcastle (Callaghan Campus), and the average air pressure of 1012 hPa was taken into calculation.

The Figure 5 above shows the effect of temperature rise on local refraction coefficient in four distinct layers according to assumptions of VTG (Section 2.3). It is worthwhile to mention here concave refraction is related to negative, and convex curvature refers to positive local refraction, while Figure 5 below compares the refracted zenith angle (") within the assumed domain of temperature.

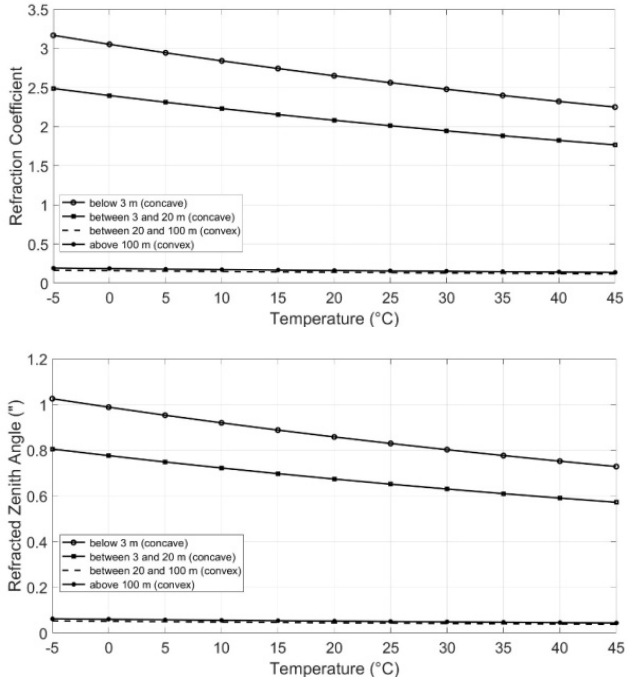

Figure 5. above: Temperature vs. local refraction coefficient, below: Temperature vs. refracted zenith angle (assumed slope distance is 20m)

Obviously, the refraction of propagating waves decreases with the rise in height above the Earth, as expected. For instance, for the layers over 20m, it is estimated to be close to zero, in contrast to two other lower layers whose magnitudes are considerably higher. That means the corresponding refracted zenith angle is also significant in those layers (Figure 5 below). In addition, it can be noted over approximately 20m of height from Earth's surface, refraction is expected to be constant and irrespective to the thermal instability of the near-ground layers.

Given the estimation of VTG [13,20,21] in the very close-ground layer below 1m, the anticipation can be reported even larger and more severe than those findings, particularly during the day, when the radiation of the Sun is trapped in those layers.

Table 2 shows, to be more exact, the value of refracted zenith angle w.r.t the single change of temperature in the near-ground layer (i.e., maximum refraction coefficient (-0.5) on sunny days and minimum in case of cooling off terrain (0.2)). The ratio of lines in Figure 4 depicts the approximate linear behaviour of refraction change, meaning that identical value for refracted zenith angle will be introduced as a result of each centigrade change temperature.

Table 2. Refracted zenith angle in near-ground layer

Refraction Coefficient	Refracted Zenith Angle $(arcsec/℃)$	Correction $(\mu m/℃)$
Max Refraction	0.006	-0.57
Min Refraction	-0.003	0.3

3.1.2. Atmospheric Pressure Analysis

In this analysis, the atmospheric pressure P is increased and temperature T is assumed as a constant value (by a step size of 20 hPa) . The assumed pressure range analyses are from 900 to 1100 hPa. Moreover, the average temperature of Newcastle in January 2023 was applied[1]. In Figure 6, negative and positive values refer to concave or convex bending ray.

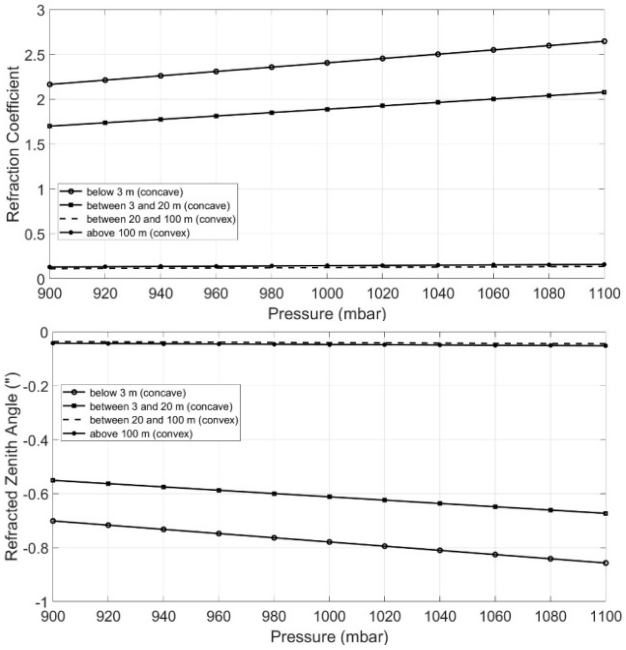

Figure 6. above: Pressure vs. local refraction coefficient, below: Pressure vs. refracted zenith angle

Unlike temperature analyse, the refraction experiences the increasing trend by the rise in atmospheric pressure (Equation 13). The variation of atmospheric pressure on refraction coefficient and corresponding refracted zenith angle is smaller than temperature change (Table 3).

Table 3. Refracted zenith angle in near-ground layer

Refraction Coefficient	Refracted Zenith Angle $(arcsec/℃)$	Correction $(\mu m/℃)$
Max Refraction	-0.0008	0.075
Min Refraction	0.0004	-0.04

From Table 2 and Table 3, it can be inferred that the main influence of refraction happens on sunny days by means of negative VTG.

The differences between layers in Figure 4 and Figure 5 clearly illustrate that the effects of the atmosphere on zenith angle by increasing the height become constant and irrelevant of the distribution of the atmosphere and more importantly negligible, while the similar influences due to the densely and erratically distribution of atmosphere in a few meters above the Earth's surface are relatively substantial. It leads to the important investigation which is implementing more complex local refraction of coefficient

between layers (i.e., when the beam ray passes from lowest to highest layers) does not make a major sense in refracted zenith angle since the main influences are derived from the lowest layers below 3 m.

The remaining questions are: what could the effect of refraction be at longer range? And what will occur if multiple variations in atmospheric conditions take place? So far, the simulated refracted zenith angle has separately been calculated based on very short range of 20 m. It is expected the effect of slope range with the existence of both factors (Equations 19 and 21) should be the same as a scale.

To better address the atmospheric variation on refracted zenith angles under the real condition of atmosphere, taking the Equations 14 and 19 into account, and merging these equations,

$$dz = \frac{S}{2R}\left[484.12\frac{P}{T^2}\left[0.0342+\left(\frac{\partial T}{\partial h}\right)\right]\right] \quad (22)$$

with slope distance $S\ (m)$, the radius of Earth $R\ (m)$, atmospheric pressure $P\ (hPa)$, air temperature $T\ (K)$, and vertical temperature gradient $\frac{\partial T}{\partial h}\ (^0K/m)$.

By partials differentials w.r.t variables of atmospheric parameters,

$$d(dz) = \frac{\partial(dz)}{\partial T}dT + \frac{\partial(dz)}{\partial P}dP \quad (23)$$

Therefore,

$$\frac{\partial(dz)}{\partial T} = -\frac{S}{R}\left[484.12\frac{P}{T^3}\left[0.0342+\left(\frac{\partial T}{\partial h}\right)\right]\right] \quad (24)$$

$$\frac{\partial(dz)}{\partial P} = \frac{S}{2R}\left[484.12\frac{1}{T^2}\left[0.0342+\left(\frac{\partial T}{\partial h}\right)\right]\right] \quad (25)$$

Considering the real atmospheric condition of Newcastle in January approximately $t = 33\ ℃$ and $P = 1012\ hPa$, mean Earth's radius of 6371000 m, and maximum value of VTG, the following Equation will be obtained for near-ground atmosphere below 3 m:

$$\frac{d(dz)_{[arcsec]}}{S_{[m]}} = \begin{bmatrix} 0.00026_{[arcsec]}dT_{[\ or\ ^\circ K]} \\ -0.00004_{[arcsec]}dP_{[hPa]} \end{bmatrix}_{[arcsec]} \quad (26)$$

The coefficients were all converted into arcseconds. Their changes w.r.t the variation of temperature, pressure and slope distance introduce total variation in refracted zenith angle (Equation 26).

In the arguments above, maximum estimated VTG in lowest layer on sunny days, has been assumed, although [13] noted that it is crucial to take the accurate principle to function VTG whose fluctuations can impose the main deviations in zenith angle measurements in lower layers (Equations 24 and 25). Therefore, determination of coefficient refraction under uncontrolled atmospheric conditions is strongly recommended (discussed in next Section).

As it is clearly shown, the effects of variations in atmospheric conditions over 20 m are quite negligible, constant, and irrelevant to the effects of atmosphere. It shall be major concern for larger ranges. Later, the calculation of VTG and corresponding local refraction coefficient under the uncontrolled environment from real datasets will be presented.

4. Data Analysis and Discussion

In order to validate the results obtained from the simulated datasets analysis, and importantly to determine the VTG under uncontrolled environment during the fieldwork measurement for our updates, real datasets were acquired in the vicinity of University of Newcastle, Callaghan campus on two separate timeslots (the 11th and 17th of January 2023) to verify VTG under two varying atmospheres. The observations were collected on four benchmarks with known coordinates located in the campus namely, PM 58000, PM 58001, PM 58002, and PM 58003 (Figure 7) (the detailed coordinates, their relevant projection systems and accuracy are listed in Appendix (Table A)).

All observations were obtained with the aid of the most accurate total station available at the university (MS60 Leica Total Station) whose angular accuracy is 1", as reported by Leica Geosystem manufactory. The instrument is able to adjust the zenith angle measurements by refraction of $+0.13$.

Figure 7. above: Four known benchmarks shown; MS60 was levelled on the PM 58000 pillar, below: The photo taken from the pillar PM 58001 (as Newcastle Test Baseline)

The height of pillar was measured by the tape with 1 mm accuracy which was 1380 mm. Therefore, the

measurements were carried out over $50\,cm$ above the ground clearness, and it is expected the local refraction will be in the lowest atmosphere (up to 3m).

The atmospheric conditions were recorded by distribution of four thermo-meter and baro-meters sensors (Figure 8). The CEM DT-3321 Hygro-Thermo-meter produced by CEM manufactory was equipped to measure temperature into 0.1 ℃ accuracy[2] (Further specifications are available through the link). The barometers which were applied were Altimeter 8 in 1 Electronic Digital Multifunction Barometer produced by Altimeter manufacturer which can sense the atmospheric pressure with lowest uncertainty of $0.1\,hPa$. Further information about the products is available [3]. In terms of accuracy, both can fulfil our measurements expectations.

Figure 8. Thermo-meters and barometers used to record the temperature and pressure during measurements

The observations on the first day were completed during the day from 11 am to 3 pm when the temperature can reach its highest peak. Also, the warm-up effects were considered at the initial point (e.g., measurement was started 20 – 25 minutes after the instrument was switched on), and refraction coefficient was switched off.

The atmospheric variations are outlined in Table 4, and angle measurements averaged from 12 times observation for each angle are summarised in Table 5.

Table 4. Atmospheric observations close to every station

Points	Temperature (℃)	Pressure (hPa)
PM 58000	29.3 - 32.4	1012.4 -1013.3
PM 58001	29.3 - 32.4	1011.4 - 1012.4
PM58002	30 - 33.2	1013.3 – 1014.2
PM 58003	29.5 - 34.6	1010.6 - 1010.8

Table 5. Calculated, measured angles and their residuals from each point

Known points (PM 5800-)	Calculated values		Measured values	Residuals
	Range	Zenith angle	Zenith angle *	
00 - 01	42.216	92° 22′ 40"	92° 21′ 2"	0° 1′ 38"
01 - 00		87° 37′ 20"	87° 38′ 34"	−0° 1′ 14"
00 - 02	385.322	91° 20′ 36"	91° 20′ 36"	0° 0′ 0"
02 - 00		88° 39′ 24"	88° 39′ 45"	−0° 0′ 21"
00 - 03	611. 021	91° 0′ 5"	91° 0′ 12"	−0° 0′ 6"
03 - 00		88° 59′ 55"	89° 0′ 14"	−0° 0′ 19"
01 - 02	343.113	91° 12′ 58"	91° 13′ 8"	−0° 1′ 50"
02 - 01		88° 47′ 2"	88° 47′ 10"	−0° 0′ 7"
01 - 03	568.817	90° 53′ 57"	90° 54′ 6"	−0° 1′ 51"
03 - 01		89° 6′ 3"	89° 6′ 12"	−0° 0′ 9"

* The measured zenith angles are averaged based on 12 repetitions at each station (detailed calculations will be used in least square).

2 https://www.cem-instruments.com/en/product-id-917
3 https://suncompany.com/products/altimeter202.

The redundant Least Square Adjustment (LSA) was implemented on MATLAB to estimate the vertical temperature gradient (VTG):

$$Y + e = A\,X \tag{27}$$

(i.e., Y is observation matrix (residuals of 120 observations), e is assumed other types of bias errors, and A is design matrix (derivation of each observation equations w.r.t the unknowns), and X is unknown matrix.

The observation equations will be given by:

$$dz + e = \frac{S}{2R}\left[484.12\frac{P}{T^2}\left[\left(\frac{\partial T}{\partial z}\right) + (0.0342)\right]\right] \tag{28}$$

The weight matrix P which is the inversion of variance covariance matrix of observations (with assumption of uncorrelated observations (zero covariance)):

$$P = C_y^{-1} = \frac{1}{\sigma_z^2} I_{120\times120} \tag{29}$$

Finally, LSA can be rewritten as follows:

$$X = (A^T PA)^{-1} A^T PY \tag{30}$$

The final estimation of VTG on the first day dataset is $-0.58\ ^0K/m$. It is expected due to the Sunny days, the absorption of the Sun's radiation is trapped into atmosphere and leads to the negative VTG.

Reference [1] recommended, in order to accurately measure refracted range, the refractive index is calculated for both terminals and the mean is taken. Reference [11] has already applied this approach for refracted range. Here, the estimation as the result of both approachs is the identical (e.g., between -0.57 and $-0.6\ ^0K/m$).

In order to verify this amount under different weather conditions, the second datasets were carried out with the same measurement configuration and the same number of repetitions for angle measurement (on 17th January between 7 pm and 10 pm). Atmospheric temperature dropped, as expected. Similar to the first day observations, the entire observations can be found in Appendix (Table B and C).

Given the different condition of atmosphere and new datasets of angle observations, the VTG will results in $-0.56\ ^0K/m$.

Thus, the maximum refraction coefficient will be expected to be within -0.5 to $-0.6\ ^0K/m$ for the lowest layer (up to $3\,m$) where the terrestrial surveying measurements are mostly collected.

Hence, the updated refraction coefficient model (Equation 14) will be presented as follows:

$$k = -274\frac{P}{T^2} \tag{31}$$

This is the maximum refraction coefficient might occur into atmosphere in lowest layer. Considering the standard condition of atmosphere ($t_{st} = 33$ ℃ and $P_{st} = 1012\ hPa$) defined by [1], and the condition of Newcastle, mentioned earlier, under which observations were carried out, the refraction coefficient will be -3.3 and -2.9, respectively. It certainly illustrates the assumption of $+13$ for most of terrestrial surveying instruments by default will not definitely be correct.

To conclude, the updated vertical temperature gradient will be slightly higher than those based on approximated values (Section 2.3). There are a number of reasons contributing to this difference:

i. The first reason is there is a minor variation between simulated (controlled), and the real observation of atmosphere, although these are insignificant and irrespective of the variations in temperature only, meaning that there are a number of other meteorological factors responsible for VTG.
ii. The employing of estimated VTG (Section 2.3) only corresponds to the average adiabatic conditions which are particularly not representative of most engineering types of measurements made close to the ground lower than half meter height where the heating effects are predominate [10]. The proper configuration for measuring VTG always is recommended.
iii. Thirdly, the presence of other variables of the atmosphere such as humidity especially in the area of Newcastle is also likely to be important for assumption of VTG and coefficient of refraction.

As already argued, the complexity of VTG in different layers can be well satisfied by the proper configuration of measurements in lowest and ultra-lowest layers. Otherwise, the other possibility would be to eliminate the uncertain value of VTG in refracted zenith angle model with the aid of other meteorological approaches.

5. Conclusion

Nowadays, accurate geodetic measurements are quite demanding for project managers. The accuracy of laser-based measurements like any other geodetic measurements is certainly affected by different variables especially atmospheric changes. This research aimed to reveal the updated model for atmospheric effects on zenith angle measurements with the aid of the local refraction coefficient via considering the vertical temperature gradient as a major element in different layers of atmosphere above the Earth's ground. The influences of two constitutions of the atmosphere including air temperature and atmospheric pressure were analysed although several other elements of the atmosphere influence the direction of the laser beam which can be assumed to be insignificant.

The temperature variation has brought the dominating impact on refracted zenith angle over longer range. Additionally, the rigorous algorithm to estimate VTG is still in question, due to the fact that it is unlikely to be directly measured. The approximation of VTG at five atmospheric layers have been executed and acknowledged the more complex model between layers will not be seriously important. For the sake of that, the updated value for VTG in lowest layer (near-ground layer) through LSA under the real atmospheric and redundant zenith angle observations have been implemented.

There have been several arguments for further investigations as future works. Firstly, it is strongly suggested to establish the appropriate approach to meteorologically determine horizontal and vertical temperature gradient (HTG) or (VTG) (i.e., both affecting their corresponding directions) and their correlations rather than applying their approximated values [7]. Finally, all assumptions were discussed in the layers up to a few meters above the Earth's surface where the atmospheric conditions can be severe and unexpected for terrestrial measurements. In case the zenith angles are measured at a height above $100\,m$ from the Earth by airborne or spaceborne instruments, vertical refraction through passing different layers from space to the ground will be significantly different area of research.

6. Appendix

Table A. Known coordinates of the points (pillars).

Points	Easting	Northing	Height
PM 58000	378021.410	6360300.214	26.443
PM 58001	379054.567	6360074.142	24.690
PM 58002	379324.231	6359862.115	17.407
PM 58003	379051.668	6359722.611	15.762

The coordinates were calculated on Map Grid of Australia (MGA) which uses Easting and Northing coordinates. Their projection system is based on Universal Transverse Mercator (UTM) and in a specified projection zone of 56. The heights are based on the Australian Height Datum (AHD), which closely approximates Mean Sea Level (MSL). These are the common projection systems used in New South Wales (NSW) in Australia.

Secondly, detailed observations including atmospheric and angle measurements gathered on the second day are shown in Tables B and C, respectively.

Table B. Atmospheric observations close to every station

Points	Temperature (℃)	Pressure (hPa)
PM 58000	15.4 - 19	1012.4 -1013.3
PM 58001	16.3 - 21	1011.3 - 1012.1
PM58002	19 - 20	1013.3 – 1014.2
PM 58003	17 - 22	1010.7 - 1010.8

Table C. Observation angles from each point.

Known points (PM 580-)	Measured values	Residuals
	Zenith angle	
00 - 01	92° 22′ 20"	0° 0′ 20"
01 - 00	87° 38′ 36"	−0° 1′ 16"
00 - 02	91° 20′ 25"	0° 0′ 11"
02 - 00	88° 39′ 45"	−0° 0′ 21"
00 - 03	91° 0′ 58"	−0° 0′ 53"
03 - 00	88° 59′ 20"	0° 0′ 35"
01 - 02	91° 12′ 40"	0° 0′ 18"
02 - 01	88° 47′ 02"	0° 0′ 0"
01 - 03	90° 54′ 1"	−0° 0′ 04"
03 - 01	89° 6′ 12"	−0° 0′ 9"

Acknowledgements

This work was a part of Master research at the University of Stuttgart, but it has been entirely improved at the University of Newcastle as a part of ongoing PhD studies.

Statement of Competing Interests

The authors have no competing interests.

References

[1] Reuger, J., Electronic Distance Measurements (3rd Edition), Springer-Verlag, 1990.

[2] Bomford, B. G., Geodesy, Oxford, 1962.

[3] Johnston, A., "Lateral Refraction in Tunnels," *Survey Review*, pp. 31:242, 201-220, 1991.

[4] Torge, W., Geodesy, Walter de Gruyter, Berlin, New York, 2001.

[5] Nikolitsas, K., and Lambrou, K., "A Methodology for Correcting Refraction in Vertical Angles for Precise Monitoring in Tunnels.," in *In. Proc. of 4th Joint International Symposium on Deformation Monitoring (JISDM).* , Athens, Greece, 2019.

[6] C. Hennes. M., Donicke. R., and Christ. H., "Zur Bestimmung der temepraturgradienteninduzierten Richtungsverschwenkni beim Tunnelvortrieb," p. Vol. VPK. 8/99, 1999.

[7] Brunner, F. K., Geodetic Refraction: Effects of Electromagnetic Wave Propagation Through the Atmosphere., Berlin, Heidelberg, New York, Tokyo: Spriner-Verlag, 1984.

[8] Ingensand. H., and Bockem. B., "Automatic location and pointing Techniques in local positioning systems.," in *4th Conference of Optical 3D Measurement Techniques*, Zurich, 1997.

[9] Brunner. F. K., and fraser. C., "Application of the Atmospheric Turbulent Transfer Model (TTM) for the Reduction of Microwave FDM," *Journal of Geodesy, Photogrammetry and Surveying* , 1977.

[10] Dodson, J., "Refraction Effects on Vertical Angle Measurements.," *Survey Review*, 1985.

[11] Sabzali, M., "IMPROVEMENT THE MODELLING OF ATMOSPHERIC EFFECTS FOR ELECTRONIC DISTANCE MEASUREMENT (EDM): ANALYSIS OF AIR TEMPERATURE, ATMOSPHERIC PRESSURE ANDRELATIVE HUMIDITY OF AIR," *GEodesy and Cartography*, 2022.

[12] "International Association of Geodesy [IAG]," in *IAG Resolutions at the XXIIth General Assembly*, Birmingham , 1999.

[13] Kharagani, M., "Propagation of Refraction Errors in Trigonometric Height Traversing and Geodetic Levelling," *PhD Thesis at Univerity of New Brunswick, Canada, published*, 1987.

[14] Angus-Leppan, A., "Geodetic Refraction," *Geophysics. Encyclopedia of Earth Science. Springer.*, 1989.

[15] Moreno, B. S., Villamayor, G. A. L., and Talens, G. P., "Practical Formulas for the Refraction Coefficient," *Journal of Surveying Engineering*, pp. 140(2): 1-5, 2014.

[16] Friedli. E., Presl. R., and Wieser. A., "Influence of atmospheric refraction on terrestrial laser scanning at long range," in *Proceedings of 4th Joint International Symposium on Deformation Monitoring (JISDM)*, Athens, Greece, 2019.

[17] Kukkamaki, T. J., "Ober die nivellitische Refraktion," *Publication of the Finnish Geodetic Institute,* , Vols. No. 25, Helsinki, Finland, 1938.

[18] Reissmann, G., "Untersuchungen zur Ausschaltung des einflusses der Vertikalrefraktion beim Präzisionsnivellement.," *Wiss. Berichte, Folge V, Vermessung,* , Vols. heft 2, Berlin, 1954.

[19] Heer. R., and Niemeier. W., "Theoretical models, practical experiments, and the numerical evaluation of refraction effects in geodetic levelling," *Third International Symposium on the North American Vertical Datum, Natl. Oceanic Atmos. Admin., Silver Spring, Md.*, pp. 321-342, 1984.

[20] Brocks, J., "Meteorologische Hilfsmittel für die geodätische Höhenmessung," *Z. Vermess.,*, pp. 3, 71-76; 4, 110-116, 145-152, 1950.

[21] Hübner, E., "Einfluss der terrestrischen Refraktion auf den Laserstrahl in bodennahen Luftschichten,," *Vermessungstechnik,* , vol. 25(10)., p. 349-353., 1977.

[22] Hirt. C., Guillaume. S., Wisbar. A., Burki. B., and Sternberg. H., "Monitoring of the refraction coefficient in the lower atmosphere using a controlled setup of simultaneous reciprocal vertical angle measurements," *Journal of Geophysical Research: Atmospheres*, vol. 115, 2010.

[23] Hennes, M., "Das Nivelliersystem-Feldprüfverfahren nach ISO 17123-2 im Kontext refraktiver Störeinflüsse,," *Allg. Vermessung*, vol. 3, p. 85-94., 2006.

[24] Ciddor, P. E., "Refractive Index of Air: New Equation for Visible and Near Infrared.," *Applied Optics*, pp. 1566-1573, 1996.

[25] Ciddor. P. E., and Hill. R. J., "Refractive index of air. 2. Group Index," *Journal of Applied Optics*, pp. 1663-1667, 1999.